

## Electronic Supplementary Information

# **Achieving ultralong directional liquid transportation spontaneously with a high velocity**

Qiankai Liu<sup>a, &</sup>, Jie Zhang<sup>a, &</sup>, Pengcheng Sun<sup>a, b, &</sup>, Jianping Wang<sup>a</sup>, Wei Zhao<sup>a</sup>,  
Guolong Zhao<sup>a</sup>, Ni Chen<sup>a</sup>, Yinfei Yang<sup>a</sup>, Liang Li<sup>a</sup>, Ning He<sup>a</sup>, Zuankai Wang<sup>c, \*</sup>,  
Xiuqing Hao<sup>a, \*</sup>

<sup>a</sup>*College of Mechanical and Electrical Engineering, Nanjing University of Aeronautics & Astronautics, Nanjing, 210016, China*

<sup>b</sup>*Department of Mechanical Engineering, City University of Hong Kong, Hong Kong, 999077, China*

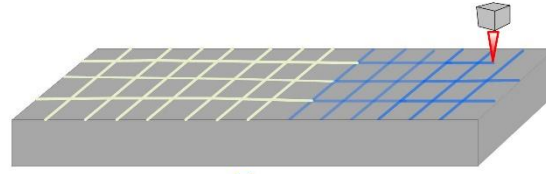
<sup>c</sup>*Department of Mechanical Engineering, The Hong Kong Polytechnic University, Hong Kong, 999077, China.*

<sup>&</sup> These authors are co-first authors.

**\*Corresponding Author**

*E-mail address:* xqhao@nuaa.edu.cn (X. Hao), zk.wang@polyu.edu.hk (Z. Wang).

**Step1:** Preparation of a gradient hydrophobic background at a gradient scanning speed



Reduced surface energy

**Step2:** Machining a streamlined cascaded super-hydrophilic divergent channel

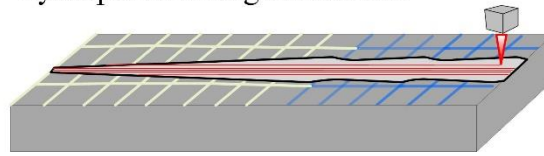


**Fig. S1** Schematics illustrating of the fabrication process of CWP

**Table S1** Laser parameters for the preparation of different wetting gradient backgrounds ( $k = 0, 0.20, 0.30$  and  $0.35^\circ \text{ mm}^{-1}$ )

Laser parameters	Scanning speed (mm/s)	Hatching loop	Power (W)	Frequency (kHz)	Hatching distance ( $\mu\text{m}$ )
Value ( $k = 0^\circ \text{ mm}^{-1}$ )	200	Vertical:1; Horizontal:1;	16	20	80
Value ( $k = 0.20^\circ \text{ mm}^{-1}$ )	200, 250, 300, 350, 400, 450, 500, 550, 600, 650, 700, 750, 800, 850, 900, 950, 1000, 1050, 1100, 1150	Vertical:1; Horizontal:1;	16	20	80
Value ( $k = 0.30^\circ \text{ mm}^{-1}$ )	200, 300, 400, 500, 600, 700, 800, 900, 1000, 1100, 1200, 1300, 1400, 1500, 1600, 1700, 1800, 1900, 2000, 2100	Vertical:1; Horizontal:1;	16	20	80
Value ( $k = 0.35^\circ \text{ mm}^{-1}$ )	200, 400, 600, 800, 1000, 1200, 1400, 1600, 1800, 2000, 2200, 2400, 2600, 2800, 3000, 3200, 3400, 3600, 3800, 4000	Vertical:1; Horizontal:1;	16	20	80

**Table S2** Laser parameters for the preparation of all super-hydrophilic channels

Laser parameters	Scanning speed (mm s <sup>-1</sup> )	Hatching loop	Power (W)	Frequency (kHz)	Hatching distance (μm)
Value	1	2	20	20	30

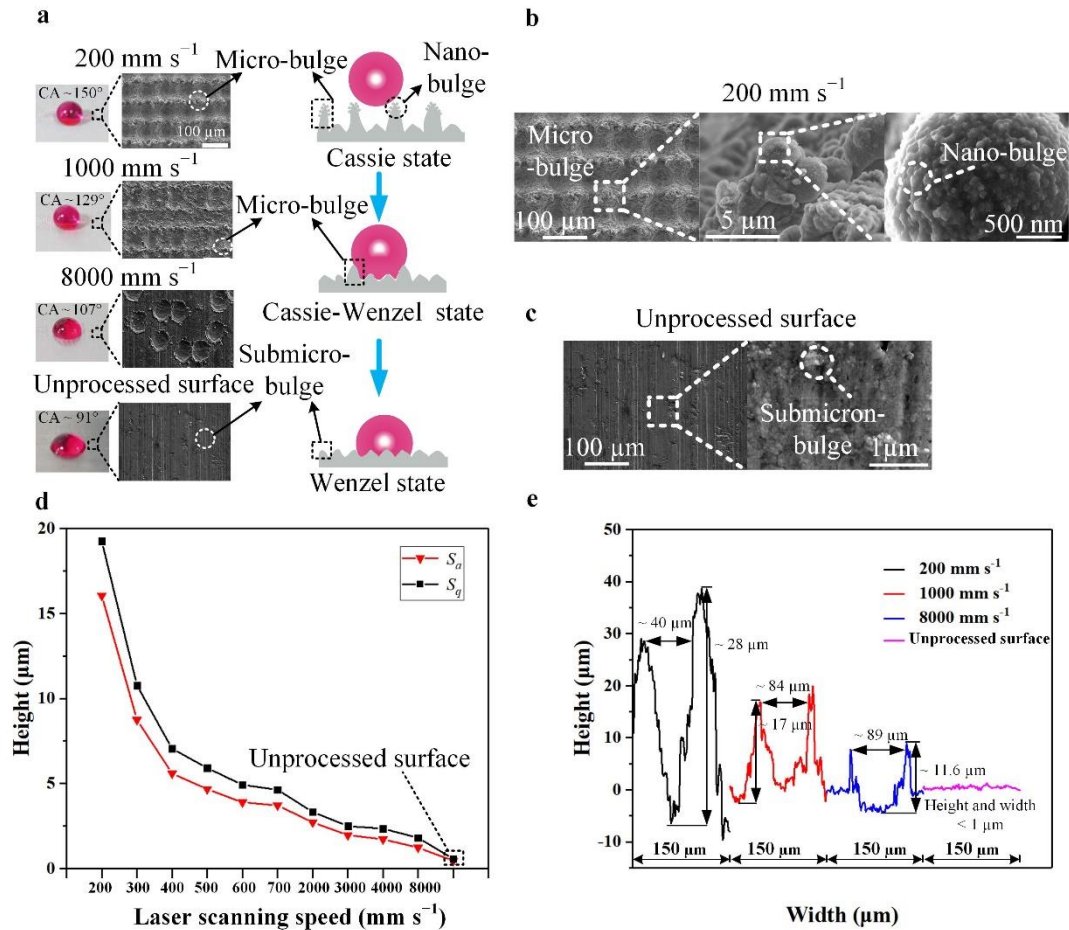


**Fig. S2** The relationship between surface structure and wettability of backgrounds, detailed drawings of SEM images, and the sizes and surface roughness of backgrounds fabricated at different laser scanning speeds. (a) The relationship between surface structure and wettability of backgrounds fabricated at different laser scanning speeds. (b) SEM images of the background which were fabricated at 200 mm s<sup>-1</sup>. (c) SEM images of the rough surface. (d) The effect of laser scanning speeds on surface roughness, where S<sub>q</sub> and S<sub>a</sub> are the standard deviation and the mean of height of surface structures, respectively. (e) The sizes of surface profiles which were prepared at 200, 1000, and 8000 mm s<sup>-1</sup> and the size of the surface profile of the rough surface.

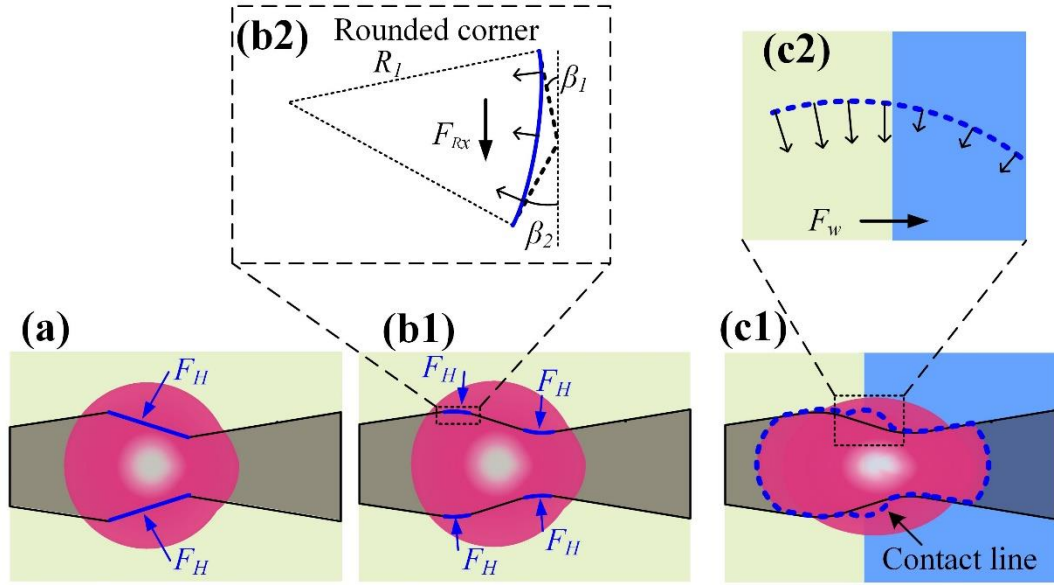


**Fig. S3** The hysteresis resistance force  $F_H$  and the wetting gradient force  $F_w$  act at boundaries. (a) Force analysis of a drop on smooth boundaries without rounded corners. (b) Force analysis of a drop on rounded corners with radius  $R_l$ . (c) Force analysis of a drop on the wetting gradient background.

**Table S3** Contact angles  $\theta$  and sliding angles  $\alpha$  of backgrounds

fabricated at different laser scanning speeds		
Laser scanning speed ( $\text{mm s}^{-1}$ )	$\theta$ ( $^\circ$ )	$\alpha$ ( $^\circ$ )
200	150.16	5.61
300	149.16	15.51
400	146.86	25.43
500	139.06	56.43
600	134.06	Pinning
700	133.5	Pinning
2000	117.18	Pinning
3000	114.18	Pinning
4000	111.86	Pinning
8000	106.94	Pinning
Rough surface	91.46	Pinning

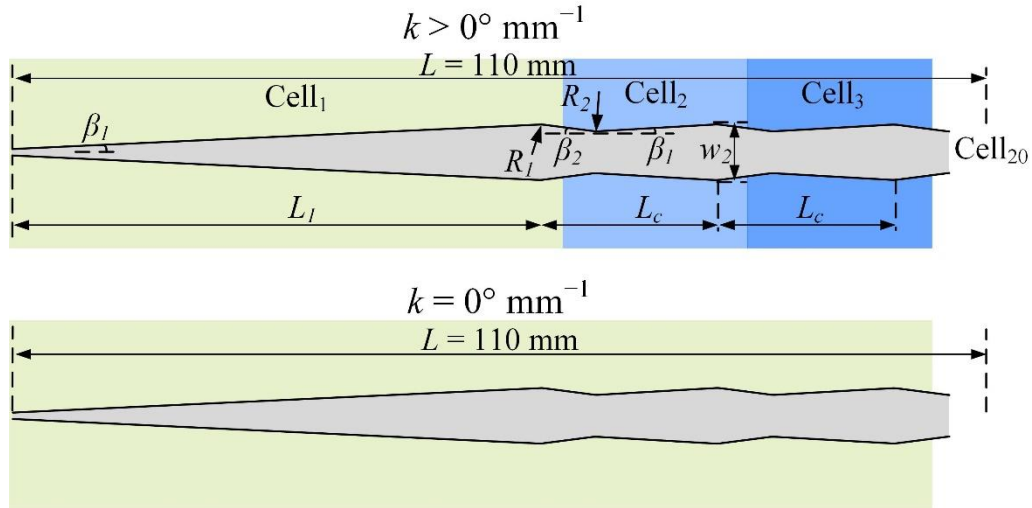


**Fig. S4** Detailed design drawing of CWPs with different average wetting gradients. The CWP with  $k = 0^\circ \text{ mm}^{-1}$  is composed of a super-hydrophilic channel and a uniform wetting background. The CWP with  $k > 0^\circ \text{ mm}^{-1}$  is composed of a super-hydrophilic channel and a gradient hydrophobic background consisting of 20 cells. The geometrical parameters of all super-hydrophilic channels are the same.

**Table S4** Geometric parameters of the smooth cascaded divergent channel

Geometric parameters	Length $L_1, L_c, L$ (mm)	Wedge angle $\beta_1$ ( $^\circ$ )	Transition angle $\beta_2$ ( $^\circ$ )	Width $w_2$ (mm)	Fillet radius $R_1, R_2$ (mm)
Value	15, 5, 110	1.5	12	1	2, 4

**Table S5** Wetting performances at different cells of backgrounds with different average wetting gradients ( $k = 0.20, 0.30, \text{ and } 0.35^\circ \text{ mm}^{-1}$ )

Parts of backgrounds	$0.20^\circ \text{ mm}^{-1}$		$0.30^\circ \text{ mm}^{-1}$		$0.35^\circ \text{ mm}^{-1}$	
	$\theta$ ( $^\circ$ )	$\alpha$ ( $^\circ$ )	$\theta$ ( $^\circ$ )	$\alpha$ ( $^\circ$ )	$\theta$ ( $^\circ$ )	$\alpha$ ( $^\circ$ )
Cell <sub>1</sub>	150.16	5.61	150.16	5.61	150.16	5.61
Cell <sub>2</sub>	149.66	7.5	149.16	15.51	146.86	25.43
Cell <sub>3</sub>	149.16	15.51	146.86	25.43	134.06	pinning
Cell <sub>4</sub>	148.11	21.47	139.06	56.43	131.84	pinning
Cell <sub>5</sub>	146.86	25.43	134.06	pinning	129.22	pinning
Cell <sub>6</sub>	143.96	35.33	133.5	pinning	128.04	pinning
Cell <sub>7</sub>	139.06	56.43	131.84	pinning	125.62	pinning
Cell <sub>8</sub>	136.66	81.26	130.3	pinning	122.38	pinning
Cell <sub>9</sub>	134.06	pinning	129.22	pinning	118.88	pinning
Cell <sub>10</sub>	133.88	pinning	128.53	pinning	117.18	pinning
Cell <sub>11</sub>	133.5	pinning	128.04	pinning	116.45	pinning
Cell <sub>12</sub>	132.57	pinning	127.34	pinning	115.72	pinning
Cell <sub>13</sub>	131.84	pinning	125.62	pinning	114.99	pinning
Cell <sub>14</sub>	131.32	pinning	124.21	pinning	114.26	pinning
Cell <sub>15</sub>	130.8	pinning	122.81	pinning	114.18	pinning
Cell <sub>16</sub>	130.28	pinning	121.41	pinning	113.716	pinning
Cell <sub>17</sub>	129.76	pinning	120.01	pinning	113.252	pinning
Cell <sub>18</sub>	129.24	pinning	118.61	pinning	112.788	pinning
Cell <sub>19</sub>	128.72	pinning	117.18	pinning	112.324	pinning
Cell <sub>20</sub>	128.26	pinning	117.02	pinning	111.86	pinning

As can be seen from Table S5, the contact angles of Cell<sub>1</sub>-Cell<sub>20</sub> of backgrounds with different average wetting gradients ( $k = 0.20, 0.30, \text{ and } 0.35^\circ \text{ mm}^{-1}$ ) range from  $150.16^\circ$  to  $128.26^\circ$ ,  $150.16^\circ$  to  $117.02^\circ$  and from  $150.16^\circ$  to  $111.86^\circ$ , respectively. The calculation processes of  $k$  are as follows:  $k = 0.20^\circ \text{ mm}^{-1}$ :  $(150.16^\circ - 128.26^\circ) / 110 \text{ mm} \approx 0.20^\circ \text{ mm}^{-1}$ ;  $k = 0.30^\circ \text{ mm}^{-1}$ :  $(150.16^\circ - 117.02^\circ) / 110 \text{ mm} \approx 0.30^\circ \text{ mm}^{-1}$ ;  $k = 0.35^\circ \text{ mm}^{-1}$ :  $(150.16^\circ - 111.86^\circ) / 110 \text{ mm} \approx 0.35^\circ \text{ mm}^{-1}$ . In addition, the contact angle and the sliding angle of the background with  $k = 0^\circ \text{ mm}^{-1}$  are the same as these of Cell<sub>1</sub> of the background with  $k > 0^\circ \text{ mm}^{-1}$ .

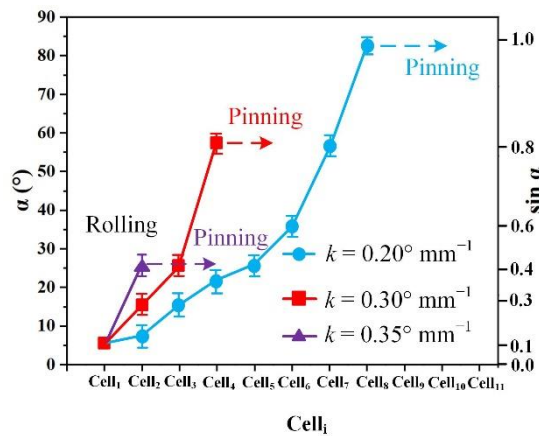


**Fig. S5** Sliding angles  $\alpha$  and their sine values  $\sin \alpha$  at different positions of different gradient hydrophobic backgrounds.

### Video S1

Transportation processes at CDU ( $\Delta\theta = 0^\circ$ ) and SDU ( $\Delta\theta = 0^\circ$ ) junctions with  $\frac{w_1}{w_2} = 0.14$  and  $w_2 = 1$  mm showing the drop being blocked and passing, respectively; this implies that the streamlined channel favors the drop passage through junctions. The video is shown at  $0.5 \times$  speed.

### Video S2

Transportation processes at SDU ( $\Delta\theta = 0^\circ$ ) and CWP ( $\Delta\theta = 58.7^\circ$ ) junctions with  $\frac{w_1}{w_2} = 0$  and  $w_2 = 1$  mm showing the drop being blocked and passing, respectively; this implies that  $\Delta\theta$  favors the drop passage through junctions. The video is shown at  $0.5 \times$  speed.

### Video S3

The transportation processes of one drop with volume of 25  $\mu\text{L}$  on different CWPs ( $k = 0, 0.20, 0.30,$  and  $0.35^\circ \text{ mm}^{-1}$ ) with  $\beta_1 = 0.15^\circ, \beta_2 = 12^\circ, L_c = 5$  mm,  $\frac{w_1}{w_2} = 0.74$  and  $w_2 = 1$  mm. Drops can achieve the transportation distance of 103 mm at  $k = 0.30^\circ \text{ mm}^{-1}$ , which is the highest of the four, and the average velocity  $v_a$  can reach  $92 \text{ mm s}^{-1}$ . The video is shown at  $0.25 \times$  speed.

### Video S4

The transportation processes of multiple drops (One drop: 5  $\mu\text{L}$ ) on the vertical long-distance straight channel with  $\beta_1 = 0.15^\circ, \beta_2 = 12^\circ, L_c = 5$  mm,  $\frac{w_1}{w_2} = 0.83$  and  $w_2 = 1.5$  mm. All drops were transported to a reservoir and the smooth cascaded divergent channel on the wetting gradient background shows the capacity of anti-gravity long-distance transportation of drops. The video is shown at  $1 \times$  speed.

### Video S5

The transportation processes of multiple drops (One drop: 5  $\mu\text{L}$ ) on the inclined straight channel with  $\beta_1 = 0.15^\circ, \beta_2 = 12^\circ, L_c = 5$  mm,  $\frac{w_1}{w_2} = 0.83$  and  $w_2 = 1.5$  mm. The uphill tilted angle is about  $3^\circ$ . All drops were transported to a reservoir. The video is shown at  $1 \times$  speed.

**Video S6**

The liquid identification processes on the horizontal four-reservoir channel with  $\beta_1 = 0.15^\circ$ ,  $\beta_2 = 12^\circ$ ,  $L_c = 5$  mm,  $\frac{w_1}{w_2} = 0.83$  and  $w_2 = 1.5$  mm. The continuous transportation of liquid was completed and the liquid identification experiment also can be achieved on the four-reservoir channel. The video is shown at  $1 \times$  speed.

**Video S7**

The transportation processes of one drop with volume of 25  $\mu$ L on the horizontal spiral channel with  $\beta_1 = 0.15^\circ$ ,  $\beta_2 = 12^\circ$ ,  $L_c = 5$  mm,  $\frac{w_1}{w_2} = 0.74$  and  $w_2 = 1$  mm. The drop can achieve the transportation distance of 72 mm. The video is shown at  $1 \times$  speed.